INTRODUCTION

Cobalt is much used as a catalyst both in the reduced (elementary) and oxidized state.[1-2] The application of cobalt as catalyst almost inexclusively involves at some stage reduction of a cobaltoxide phase, often as a part of the preparation methods (e.g. activation by reduction of an oxidized precursor phase into elementary cobalt) or due to reducing conditions in the actual process being catalyzed (e.g. presence of carbonmonoxide or hydrogen gas). Hence, in order to optimize the synthesis of the catalyst and its properties, and to fully understand the role of the catalyst under process conditions, it is imporant to have knowledge on the phase compositions, phase stability, property changes, crystal structure, and solid state reactions beween catalyst components (e.g. metal component and supporting oxide) during catalyst preparation and application. Many catalysts consist of small amounts of catalytically interesting components highly dispersed on a solid matrix (support) and often in a poorly crystalline state. For that reason, characterization techniques which are widely used for solid state materials like X-ray and neutron diffraction, give poor results when used for catalyst characterization. However, if data for the catalyst, obtained from several different complementary techniques are compared with similar measurements for closely related and well characterized model compounds, important knowledge can usually be extracted.

One such catalyst consist of cobalt supported on γ-Al_2O_3. The catalyst is relevant for synthesis of hydrocarbons by hydrogenation of carbonmonoxide, so-called Fischer-Tropsch synthesis. Usually, the Co/γ-Al_2O_3 catalysts are added noble metals like rhenium, platinum or rhodium, and rare earth elements like lanthanum in order to improve the reduction and catalytic properties of the catalysts. Hence, during synthesis and application of Co/γ-Al_2O_3 catalysts promoted with lanthanum, reactions between La and Co with formation of La-Co-O phases and between Co and γ-Al_2O_3 with formation of Co-Al-O phases are expected, as well as reactions between La and γ-Al_2O_3. On this basis a detailed study have been conducted on model oxides in the La-Co-O and Co-Al-O systems under reducing conditions typically used for the synthesis of the catalysts, and the results are presented in this thesis.

Binary and multi component cobaltoxides typically contain divalent, $Co^{II}(d^7)$, and/or trivalent, $Co^{III}(d^6)$, cobalt. In many A-Co-O systems, phases containing cobalt in both of these valence states exist. Furthermore, Co^{II} and Co^{III} may exist in a low-, intermediate- or high-spin

configuration.[a] Hence, the diversity of phases in most cobaltoxide systems is large, which makes them very interesting with respect to studies of composition - structure - property relations.

La-Co-O

The large group of perovskite type and related materials show a large diversity in chemical and physical properties,[3] and in the literature special attention has been devoted to perovskites of the 3*d*-transition elements. For many of these materials small changes in the composition lead to major changes in the properties. In this aspect the La-Co-O system has been studied thoroughly for many decades adressing topics of fundamental interest including phase stability, crystal structure, non-stoichiometry, defect ordering, and effects of dopants. Especially, questions regarding the electronic and magnetic properties are still extensively debated in the literature like metal-insulator transitions and spin state transitions for $LaCoO_3$.[4] The discovery of high temperature superconductivity in the La-Cu-O system[5] triggered an extensive renewed interest also for the structurally and electronically closely related La-Co-O and La-Ni-O systems. Furthermore, the possible application of $LaCoO_3$ as catalyst for e.g. hydrogenation of light hydrocarbons, oxidation of carbonmonoxide and reduction of nitrogenmonoxide has attracted substantial attention.[6] The possible use of perovskite oxides, including $LaCoO_3$, for electrodes and interconnects in fuel cells have been thoroughly studied.[7]

The possible applications of oxides under reducing conditions demand thorough characterization of phase stability and induced changes in composition, crystal structure and properties. In addition, studies on simple model systems are often valuable and required in order to adress more complex multicomponent systems interesting for applications. The first four papers of this thesis focus on several open questions related to the effects of reduction on the composition, crystal structure and magnetic properties of $LaCoO_{3-\delta}$ and $La_4Co_3O_{10\pm\delta}$.

Perovskite type crystal structure, AMO_3

Throughout this thesis, the descriptions of crystal structures of the studied La-Co-O phases will refer extensively to the perovskite type crystal structure adopted by $LaCoO_3$.[8] Hence, for readers not familiar with perovskite materials it is on its place to give a short description of the perovskite type crystal structure. Perovskite type oxides have the general formula AMO_3. The ideal cubic perovskite crystal structure (space group *Pm3m*) is shown in

[a] Througout this thesis superscript Roman numerals denote the valence state of atoms regardless of the spin state. Spin states are quoted by LS (low-spin), IS (intermediate-spin) and HS (high-spin) when appropriate.

Fig. 1. The B-atoms are situated at the corners of the cubic unit cell each being octahedrally coordinated by oxygen atoms, whereas the larger A-atoms are situated in the center of the unit cell surrounded by twelve oxygen atoms. Alternatively, the perovskite type structure is described by cubic close packing of AO_3-layers, (111) planes, with B-atoms occupying the octahedral holes surrounded by oxygen. Only a few of the known perovskites adopts the ideal cubic structure. In most cases, the crystal structure are either rhombohedrally or orthorhombically distorted owing to minor atomic displacements driven by either electronic instabilities of the octahedral metal atom (e.g. Jahn-Teller distortions) or instabilities due to size mismatch between the two metal atoms leading to octahedral tilting.[9] $LaCoO_3$ adopts space group $R\bar{3}c$; a = 537.78 pm, α = 60.798 °.[8]

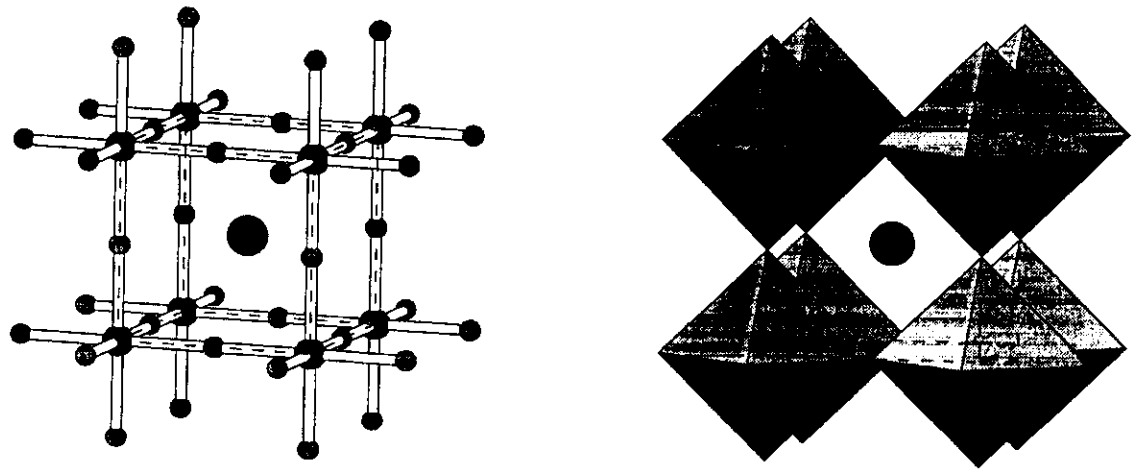

Fig. 1. Ideal cubic perovskite crystal structure, AMO_3. Unit cell (dashed lines), A (black), M (dark shaded) and O (shaded).[b] MO_6-octahedra are emphasized at right.

Ruddlesden-Popper type phases, $A_{m+1}M_mO_{3m+1}$

The Ruddlesden-Popper (RP) type crystal structures are closely related to the perovskite structure and occur for compositions with cation ratio A/M > 1. This structure type is generally described by the formula $A_{m+1}M_mO_{3m+1}$ denoting a series of compounds with m = 1, 2, 3,...., ∞. The Ruddlesden-Popper type structure was first described for $Sr_3Ti_2O_7$.[10] This series includes as end phases the K_2NiF_4-type structure with m = 1 and the perovskite structure

[b] For clarity, atom sizes are not to scale in the figures of crystal structures in this thesis.

with $m = \infty$. The ideal tetragonal crystal structures for $m = 1$, 2, and 3 are shown in Fig. 2. The typical layered arrangement of these compounds, with perovskite type slabs consisting of m layers of cornersharing MO_6-octahedra parallel to the basal plane of the unit cell stacked along the c-direction, is clearly seen. Successive perovskite type slabs are translated relative to each other giving rise to an interface where A and O atoms arrange as in the NaCl-type structure. Alternatively the general formula is written as $AO(AMO_3)_m$ in order to emphasize the layered nature of the structure and the relationship to the perovskite structure.

RP-type phases commonly exist for A-M-O systems where M is a 3*d* element. A list of selected examples are given in Table 1. There is a general trend for all these RP-systems that the physical properties show a larger degree of two-dimensional character as m become smaller. For example the resistivity of $(La_{0.4}Sr_{0.6})_3Mn_2O_7$ is much larger when measured normal to the perovskite type layers as compared to measurments parallel to the layers, whereas the resistivity for the perovskite $La_{1-x}Sr_xMnO_3$ is isotropic.[11] A second factor that has major influence on the physical properties of these materials is the valence state(s) of the transition

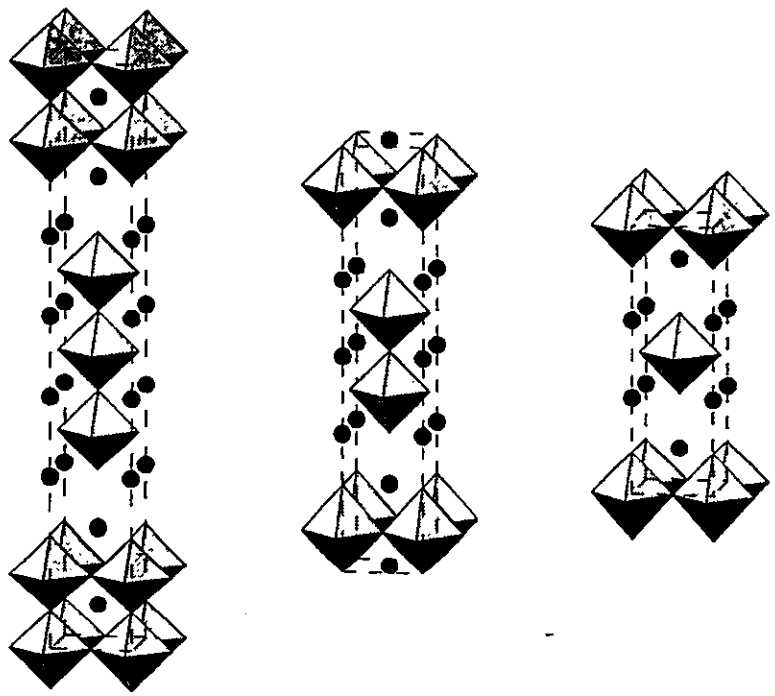

Fig. 2. Ideal tetragonal Ruddlesden-Popper type structures $A_{m+1}M_mO_{3m+1}$ for $m = 3$ (left), $m = 2$ (centre), and $m = 1$ (right). Unit cell (dashed lines), A-atoms and MO_6-octahedra shown.

Table 1. Selected examples of Ruddlesden-Popper type phases, $A_{m+1}M_mO_{3m+1}$, for the *3d*-elements (M). A separate list of references are given in the Appendix.

M	$m = \infty$ (perovskite type)	$m > 3$	$m = 3$	$m = 2$	$m = 1$ (K_2NiF_4-type)
Sc	$LaScO_3$			$SrLa_2Sc_2O_7$	$SrLaScO_4$
Ti	$CaTiO_3$		$Ca_4Ti_3O_{10}$	$Ca_3Ti_2O_7$	
	$SrTiO_3$	[a]	$Sr_4Ti_3O_{10}$ [a]	$Sr_3Ti_2O_7$	Sr_2TiO_4
	$LaTiO_3$		$K_2La_2Ti_3O_{10}$		
V	$CaVO_3$				
	$SrVO_3$		$Sr_4V_3O_{10-\delta}$	$Sr_3V_2O_7$	Sr_2VO_4
	$LaVO_3$			$Sr_{1.5}La_{1.5}V_2O_7$	$LaSrVO_4$
Cr	$CaCrO_3$				
	$SrCrO_3$				$LaSrCrO_4$
	$LaCrO_3$				
Mn	$CaMnO_3$		$La_xCa_{4-x}Mn_3O_{10}$	$A_{2-2x}B_{1+2x}Mn_2O_7$	$La_{1-x}B_{1+x}MnO_4$
	$SrMnO_3$		$(0.0 \le x \le 0.1)$	$(0.275 \le x \le 0.5)$	$(0.0 \le x \le 1.0)$
	$LaMnO_3$		$La_{1.5}Sr_{2.5}Mn_3O_{10}$	(A = La)	(B = Ca, Sr)
				(B = Ca, Sr)	
Fe	$CaFeO_3$				$LaCaFeO_4$
	$SrFeO_3$		$LaSr_3Fe_3O_{10-\delta}$	$Sr_3Fe_2O_{7-\delta}$	$Sr_2FeO_{4-\delta}$
	$LaFeO_3$				$LaSrFeO_4$
Co	$SrCoO_3$				$LaSrCoO_4$
	$LaCoO_3$		$La_4Co_3O_{10\pm\delta}$		$La_2CoO_{4+\delta}$
Ni					$LaSrNiO_4$
	$LaNiO_3$	[a]	$La_4Ni_3O_{10\pm\delta}$	$La_3Ni_2O_{7\pm\delta}$	$La_2NiO_{4+\delta}$
Cu				$Sr_2LaCuRuO_7$	$LaSrCuO_4$
	$LaCuO_3$	[a]	[a]		$La_2CuO_{4+\delta}$

[a] Only observed as stacking faults or intergrowth phase within another Ruddlesden-Popper phase.

element. An average valence state of 3.4 for manganese in $(La_{0.4}Sr_{0.6})_3Mn_2O_7$ indicates the coexistence of Mn^{III} and Mn^{IV}. The presence of such a mixed valence state for manganese is known to be essential for the giant magnetoresistance exhibited by this compound. Furthermore, for many of these RP-systems a change in the valence state of the transition

element is essential in order to stabilize the RP-type structure. That is the case for the RP-series $La_{m+1}M_mO_{3m+1}$ with M = Co and Ni, for which the formation of RP-pahses with decreasing m-value require a partial reduction of M^{III} to M^{II} as shown by the series; $LaCo^{III}O_3$ ($m = \infty$), $La_4Co^{II}Co^{III}{}_2O_{10}$ ($m = 3$), $La_2Co^{II}O_4$ ($m = 1$).[12-13] Similar effects can be obtained by aliovalent substitutions on A and M positions.

Co-Al-O

The fifth paper of this thesis reports on phase relations in the Co-Al-O system with emphasis on reduction behaviour for a series of spinel type phases, $Co_{3-x}Al_xO_4$. These are important model compounds for studies of the Co/γ-Al_2O_3 catalyst. The methods which were successfully used for synthesis and characterization of partially reduced intermediate phases in the La-Co-O system (paper 1 - 4 of this thesis), have been applied to the Co-Al-O model system and the Co/γ-Al_2O_3 catalyst.

The spinel and NaCl structure types are adopted by several phases in the Co-Al-O system which are discussed in the fifth paper. Hence, for the readers reference these two structure types are shown in Fig. 3. Both the spinel- and NaCl type structures are described by a cubic close packed (*fcc*) lattice of oxygen atoms. In the spinel type structure 1/8 of the tetrahedral and 1/2 of the octahedral interstices of the *fcc*-lattice are filled, whereas in the NaCl-type structure all octahedral sites are filled.

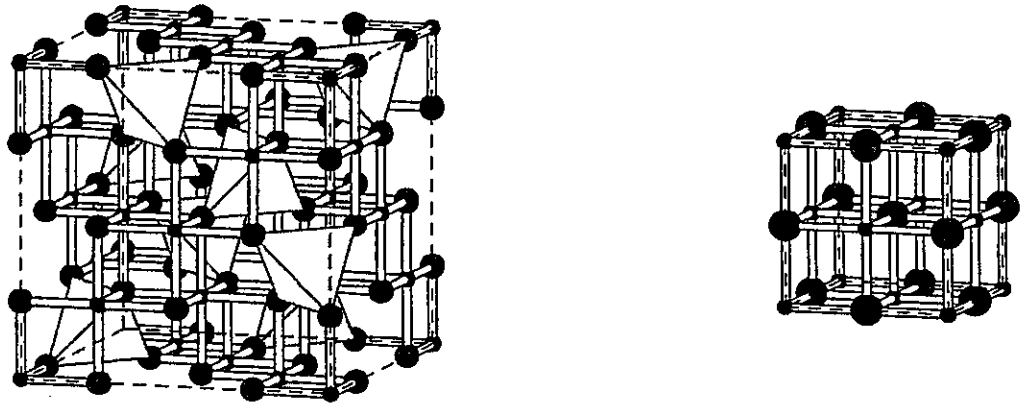

Fig. 3 (Left) Spinel type crystal structure, AB_2O_4 (space group $Fd\bar{3}m$). Unit cell (dashed lines), B (black), O (shaded), B–O bonds and AO_4-tetrahedra are shown. **(Right)** NaCl-type crystal structure, MO (space group $Fm\bar{3}m$). Unit cell (dashed lines), M (black), O (shaded) and M–O bonds are shown.

REFERENCES

1. A. A. Adesina, *Appl. Catal. A* **138**, 345 (1996)
2. S. Meijers, T. P. Pruys van der Hoeven, V. Ponec, J. P. Jacobs and H. H. Brongersma, *J. Catal.* **161**, 459 (1996)
3. F. S. Galasso, "*Perovskites and High T_C Supercondictors*", Gordon and Breach Science Publishers (1990)
4. T. Saitoh, T. Mizokawa, A. Fujimori, M. Abbate, Y. Takeda and M. Takano, *Phys. Rev. B* **55**, 4257 (1997)
5. J. G. Bednorz and K. A. Müller, *Z. Phys. B* **64**, 189 (1986)
6. L. G. Tejuca, J. L. G. Fierro and J. M. D. Tascón, *Adv. Catalysis* **36**, 237 (1989)
7. A. J. Appleby and F. R. Foulkes, *Fuel Cell Handbook*, Van Nostrand-Reinhold, New York (1989)
8. G. Thornton, B. C. Toefield and A. H. Hewat, *J. Solid State Chem.* **61**, 301 (1986)
9. P. M. Woodward, *Acta Cryst. B* **53**, 32 (1997)
10. S. N. Ruddlesden and P. Popper, *Acta Cryst.* **11**, 54 (1958)
11. Y. Moritomo, A. Asamitsu, H. Kuwahara and Y. Tokura, *Nature* **380**, 141 (1996)
12. M. Seppänen, M. Kytö, and P. Taskinen, *Scand. J. Metall.* **8**, 199 (1979)
13. K. Kitayama, *J. Solid State Chem.* **73**, 381 (1988)